Special Issue

IMI—Nonpathological Human Ocular Tissue Changes With Axial Myopia

Jost B. Jonas,[1,2] Richard F. Spaide,[3] Lisa A. Ostrin,[4] Nicola S. Logan,[5] Ian Flitcroft,[6,7] and Songhomitra Panda-Jonas[8]

[1]Department of Ophthalmology, Medical Faculty Mannheim, Heidelberg University, Mannheim, Germany
[2]Institute of Molecular and Clinical Ophthalmology Basel, Basel, Switzerland
[3]Vitreous, Retina, Macula Consultants of New York, New York, New York, United States
[4]College of Optometry, University of Houston, Houston, Texas, United States
[5]School of Optometry, Aston University, Birmingham, United Kingdom
[6]Centre for Eye Research, School of Physics and Clinical and Optometric Sciences, Technological University Dublin, Dublin, Ireland
[7]Department of Ophthalmology, Children's Health Ireland at Temple Street Hospital, Dublin, Ireland
[8]Privatpraxis Prof Jonas und Dr Panda-Jonas, Heidelberg, Germany

Correspondence: Jost B. Jonas, Universitäts-Augenklinik, Theodor-Kutzer-Ufer 1-3, 68167 Mannheim, Germany; jost.jonas@medma.uni-heidelberg.de.

Received: January 27, 2023
Accepted: February 7, 2023
Published: May 1, 2023

Citation: Jonas JB, Spaide RF, Ostrin LA, Logan NS, Flitcroft I, Panda-Jonas S. IMI—Nonpathological human ocular tissue changes with axial myopia. *Invest Ophthalmol Vis Sci.* 2023;64(6):5. https://doi.org/10.1167/iovs.64.6.5

Purpose. To describe nonpathological myopia-related characteristics of the human eye.

Methods. Based on histomorphometric and clinical studies, qualitative and quantitative findings associated with myopic axial elongation are presented.

Results. In axial myopia, the eye changes from a spherical shape to a prolate ellipsoid, photoreceptor, and retinal pigment epithelium cell density and total retinal thickness decrease, most marked in the retroequatorial region, followed by the equator. The choroid and sclera are thin, most markedly at the posterior pole and least markedly at the ora serrata. The sclera undergoes alterations in fibroblast activity, changes in extracellular matrix content, and remodeling. Bruch's membrane (BM) thickness is unrelated to axial length, although the BM volume increases. In moderate myopia, the BM opening shifts, usually toward the fovea, leading to the BM overhanging into the nasal intrapapillary compartment. Subsequently, the BM is absent in the temporal region (such as parapapillary gamma zone), the optic disc takes on a vertically oval shape, the fovea–optic disc distance elongates without macular BM elongation, the angle kappa reduces, and the papillomacular retinal vessels and nerve fibers straighten and stretch. In high myopia, the BM opening and the optic disc enlarge, the lamina cribrosa, the peripapillary scleral flange (such as parapapillary delta zone) and the peripapillary choroidal border tissue lengthen and thin, and a circular gamma and delta zone develop.

Conclusions. A thorough characterization of ocular changes in nonpathological myopia are of importance to better understand the mechanisms of myopic axial elongation, pathological structural changes, and psychophysical sequelae of myopia on visual function.

Keywords: axial myopia, high myopia, axial elongation, retinal pigment epithelium, Bruch's membrane

Axial myopia is associated with a panoply of both nonpathological and pathological histological and gross changes of the eye.[1,2] Although the etiology has not yet been described completely, axial myopia occurs when the axial length of the eye grows too long for the optics, and images focus in front of the retina. In axially myopic eyes, structural ocular changes occur as a result of axial elongation and predominantly affect tissues located posterior to the ora serrata. In this review, nonpathological ocular tissue changes associated with axial myopia are described, differentiating those related to mild to moderate myopia compared to high myopia, with a cut-off for high myopia of approximately −6.0 to −8.0 diopters (D) in refractive error and about 26.0 mm in axial length.[3]

Orbit and Ocular Shape

Emmetropic eyes are generally oblate or spherical in shape. Myopic axial elongation leads to a change in eye shape to a prolate ellipsoid.[4–11] The easiest way to geometrically explain such a change is a sagittal enlargement of a sphere's wall in the equatorial region. Recent studies have demonstrated that the density of photoreceptors and RPE cells and total retinal thickness show an axial length-associated decrease, most marked at the midpoint between the equator and posterior pole, followed by the equatorial region, suggesting that the retroequatorial region is the center of myopic eye wall enlargement.[12–14] If the center of ocular wall enlargement were located exactly at the equator, a purely

Investigative Ophthalmology & Visual Science

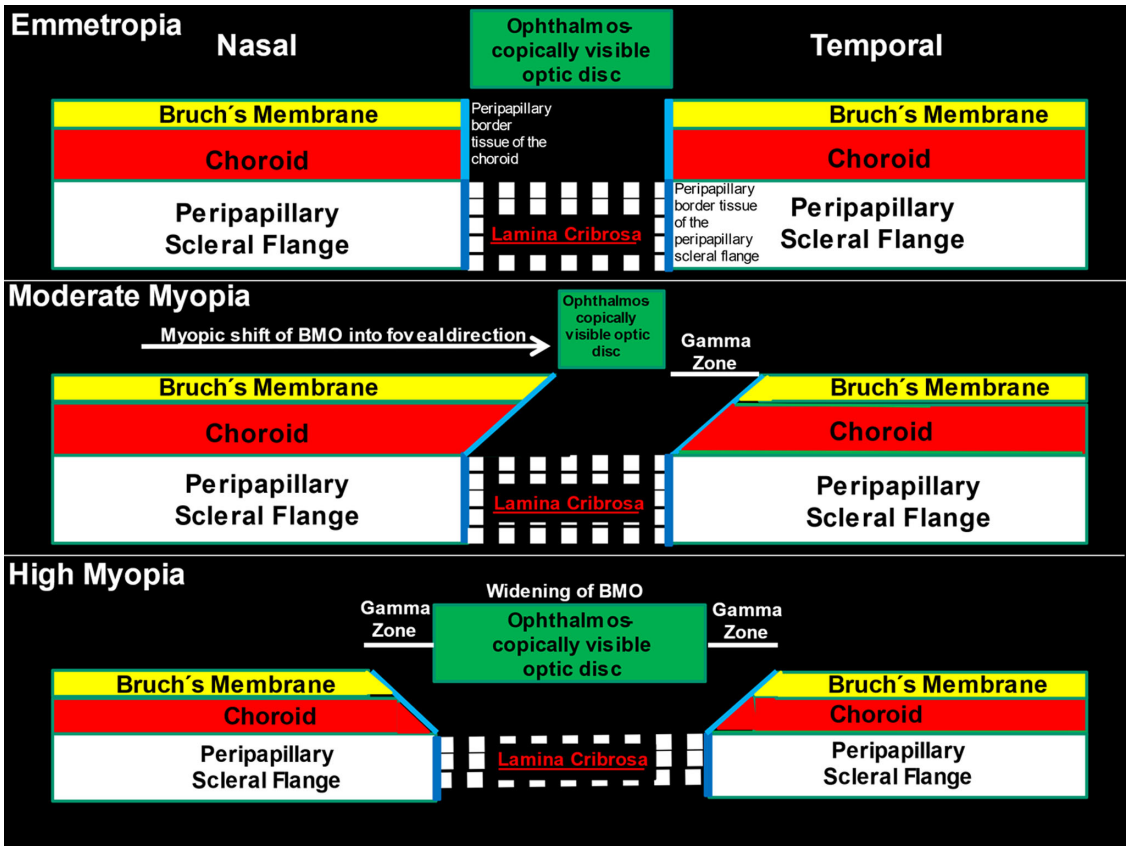

Figure 1. Scheme showing the alignment of all three ONH canal layers (BMO, choroidal opening and peripapillary scleral flange opening, spanned by the lamina cribrosa) in emmetropic eyes (*top*), the shift of BMO into the temporal direction in moderately myopic eyes (*middle*), and the widening of BMO in highly myopic eyes (*bottom*). Reprinted from Jonas JB, Jonas RA, Bikbov MM, Wang YX, Panda-Jonas S. Myopia: Histology, clinical features, and potential implications for the etiology of axial elongation. *Prog Retin Eye Res*. 2022 Dec 28:101156. Online ahead of print. © 2022 Elsevier Ltd.

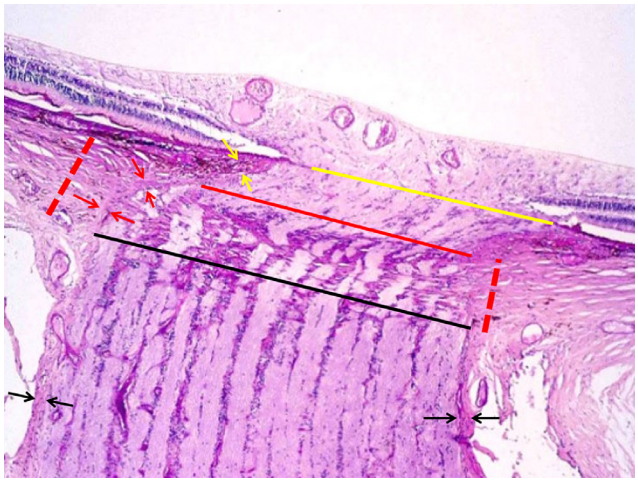

Figure 2. Histophotograph of an ONH of a moderately myopic eye, showing the three layers of the ONH canal: the BMO (*yellow line*), the choroidal opening (between the yellow line and the red line), demarcated by the choroidal peripapillary border tissue ("Jacoby") (*yellow arrows*), and the opening of the peripapillary scleral flange, covered by the lamina cribrosa (between the *red line* and the *black line*) and demarcated by the peripapillary border tissue of the peripapillary scleral flange ("Elschnig") (*red arrows*); perforated red line: peripapillary scleral flange; black arrows: optic nerve pia mater.

axial elongation would be more likely to occur. However, with the center of wall enlargement located posterior to the equator, axial elongation would be expected to occur along with an increase, to a minor amount, in the horizontal and vertical diameters of the globe, combined with a minor enlargement of the eye wall also in the pre-equatorial region. Evidence for the predominantly retroequatorial location is provided in a study investigating enucleated eyes; in eyes with an axial length of 24 mm or less, an increase of horizontal and vertical eye diameters of 0.44 mm and 0.51 mm was observed for each mm increase in axial length, respectively, and in eyes with an axial length of more than 24 mm, there was an increase in the horizontal and vertical eye diameters of 0.19 mm and 0.21 mm, respectively, for each millimeter increase in axial length.[7] This finding may also explain why axial elongation leads to an enlargement of the Bruch's membrane opening (BMO) of the optic nerve head (ONH), because the axial elongation–associated increase in the coronal diameters of the globe may increase the strain within BM in the posterior region. Increased strain within the BM may first lead to an enlargement of the BMO, followed by the development of secondary expansion defects of BM in the macular region.[15–17] A retroequatorial location of the center of the myopic enlargement of the eye wall is in accordance with observations from experimental and clinical studies in which the sensory part of the feedback mechanism regulating axial elongation has been shown to exist in the

Investigative Ophthalmology & Visual Science

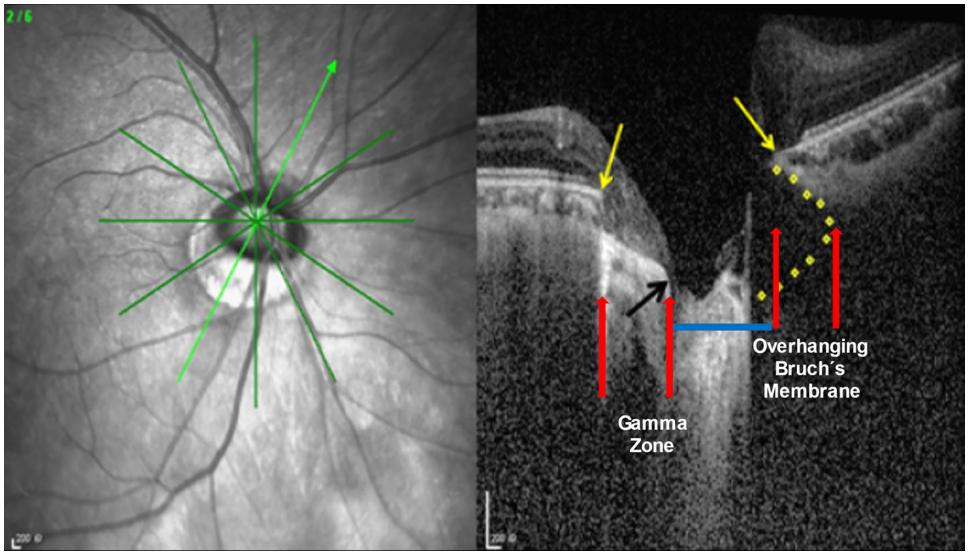

Figure 3. Optic coherence tomography image of an ONH in a moderately myopic eye, showing the intrapapillary overhanging of BM in the nasal region, the corresponding absence of BM (such as gamma zone) in the temporal inferior region, and the relatively small optic disc diameter (*blue line*), ophthalmoscopically reduced by the overhanging part of the BM; *yellow arrows*, ends of the BM; *black arrow*, central end of gamma zone.

midperipheral region of the posterior eye.[18–21] The notion of an eye wall enlargement in the retroequatorial and equatorial regions also fits with the clinical observation of a posterior shift of BMO in the foveal direction.[15–17] The BMO shift in the foveal direction explains further observations in axial myopia, including an overhanging of BM into the intrapapillary compartment (such as the compartment anterior to the lamina cribrosa and surrounded by the peripapillary border choroidal tissue) at the nasal optic disc border, an ovalization of the optic disc shape in moderately myopic eyes, and a compensatory absence of BM in the temporal parapapillary region, such as parapapillary gamma zone (Figs. 1 to 3).[15,17,22,23] Correspondingly, the optic disc–fovea distance in these eyes with a temporal gamma zone is elongated.[24]

Optic Nerve Head

The ONH consists of the ONH canal and the parapapillary region.[17] The ONH canal is the outlet for retinal ganglion cells axons (such as retinal nerve fibers) and central retinal vein and the inlet for the central retinal artery. The ONH canal wall is composed of three layers: the BMO as the inner layer, the choroidal opening as the middle layer, and the lamina cribrosa as the perforated opening in the peripapillary scleral flange as the outer layer (Figs. 1 to 3).[2,17] The ONH canal contains approximately 1.2 million nerve fibers passing through approximately 160 to 300 lamina cribrosa pores.[25,26] The central retinal vessel trunk is located in the central region of the lamina cribrosa, usually slightly decentered in the nasal upper direction.[27]

Optic Disc

The optic disc can be regarded as the ophthalmoscopically visible part of the neuroretinal rim and optic cup.[28] The optic disc shape changes from a mostly circular form in emmetropic eyes to an oval, usually vertically oval, form in moderately myopic eyes, often in association with a relatively small optic disc size.[22,28–31] A shift of the BMO in the temporal direction, leading to an overhanging of BM into the nasal intrapapillary compartment (Figs. 1 to 3), may be the reason for the optic disc change from circular to oval.[2,16,22,23] The overhanging part of BM prevents the ophthalmoscopic detectability of the optic cup in the nasal region, so that the optic disc, if defined as the ophthalmoscopically visible part of the neuroretinal rim and optic cup, gets smaller, and its shape assumes a vertical oval.[16,17,22] Another minor reason for the vertical ovalization of the optic disc shape upon ophthalmoscopy may be a perspective artefact; during axial elongation, the ophthalmoscopic view onto the optic disc changes from a mostly perpendicular angle to an oblique angle.[32] Because of this perspective, the horizontal optic disc diameter appears relatively shortened.

Although moderately myopic eyes may have a relatively small optic disc, highly myopic eyes tend to have a larger optic disc, as well as a larger ONH canal, than both moderately myopic and emmetropic eyes.[33,34] Optic disc enlargement in highly myopic eyes is associated with a lengthening and thinning of the lamina cribrosa.[35] A decreased lamina cribrosa thickness shortens the distance between the intraocular compartment, which is under IOP, and the retrobulbar compartment, which is under orbital cerebrospinal fluid pressure pressure.[36] The resulting steepening of the translaminar pressure gradient and pronounced morphological intralaminar changes, with a potential shearing effect on the lamina cribrosa pores, may contribute to the increased prevalence of glaucoma-like and/or glaucomatous optic neuropathy in high myopia.[37–41] In highly myopic eyes, stretching of the lamina cribrosa, together with a flattening of the parapapillary tissue caused by the development of parapapillary gamma zone and delta zone, leads to a flattening of the optic cup, because the spatial difference between the height of the neuroretinal rim and the depth of the optic cup is decreased.[33,34] This factor hinders the delineation of the neuroretinal rim from the

Investigative Ophthalmology & Visual Science

optic cup and is one of the reasons for increased difficulty in detecting optic nerve damage in a highly myopic ONH.[42] Optic disc enlargement in highly myopic eyes is accompanied by an enlargement of the BMO, which leads to a retraction of the nasal overhang of BM into the parapapillary region, so that a circular parapapillary gamma zone develops.[16,17,42–44]

In highly myopic eyes, the optic disc shape shows high interindividual variability.[33,34] The longest axis of the disc can be vertically or obliquely, and sometimes horizontally, oriented. In extremely myopic eyes, the optic disc may be influenced by a backward pull of the optic nerve, being potentially too short to allow a pronounced adduction of the eye with a markedly elongated axial length.[45,46] Because the optic nerve originates slightly superior and nasal in the orbit, the optic nerve pull, probably exerted by the optic nerve dura mater on its insertion line at the posterior sclera (e.g., the peripheral end of the peripapillary scleral flange), will be maximal at the temporal inferior ONH region. This would lead to a vertical rotation of the ONH, so that its shape, as assessed ophthalmoscopically, becomes vertically oval. Because the backward pull may be strongest, not exactly at the temporal ONH border, but at the temporal inferior ONH border, it may also lead to a rotation of the ONH around its sagittal axis, with the superior disc pole turning in the direction of the fovea. Such a mechanism could explain the relatively frequent finding of a sagittal ONH rotation in the direction toward the fovea.

Parapapillary Gamma Zone and Delta Zone

The three layers composing the ONH canal are aligned to each other at birth and form a mostly perpendicular angle with the sclera (Fig. 1). In adolescents and young adults with developing moderate myopia, the ONH canal assumes an oblique orientation, with the BMO located usually in direction of the fovea and the lamina cribrosa located anteriorly to it. This orientation leads to an oblique exit of the retinal nerve fibers from posterior internal-to-anterior external direction, before the nerve fibers, then within the optic nerve, bend backward in direction toward the superior nasal region of the orbit. As pointed out elsewhere in this article, the misalignment of the three ONH canal layers leads to an overhanging of BM into the intrapapillary compartment at the nasal optic disc side, and to an absence of BM in the temporal parapapillary region (Figs. 1 to 3).[16,17,23] A region without BM in the parapapillary area is termed the gamma zone (Fig. 4).[17,43,44]

The etiology for the misalignment of the ONH canal structures has remained elusive. As discussed by Lee et al.,[47] a potential mechanism could be an anterior shift of the lamina cribrosa leading to an oblique exit of the nerve fibers in posterior-to-anterior direction. The forces provoking such an anterior lamina cribrosa shift are unclear, in particular because studies have suggested that the optic nerve in axially elongated eyes may, if the eye is adducted, pull the ONH structures backward (as stated elsewhere in this article) and not forward.[45,46] An alternative mechanism is a shift of the BMO in direction of the fovea. Such a backward shift of the BMO could be produced by an enlargement of BM in the equatorial and retroequatorial region, as discussed in previous studies.[15]

Beside the misalignment of the ONH canal layers, an axial elongation–associated enlargement of the BMO is a second mechanism that may contribute to the enlargement of gamma zone.[16] Cross-sectional studies have suggested that BMO enlargement is present in eyes with an axial length of more than 26.0 or 26.5 mm (or a myopic refractive error of approximately −8.0 D).[16] The BMO enlargement leads to a retraction of the intrapapillarily overhanging BM so that a circular gamma zone develops.[44]

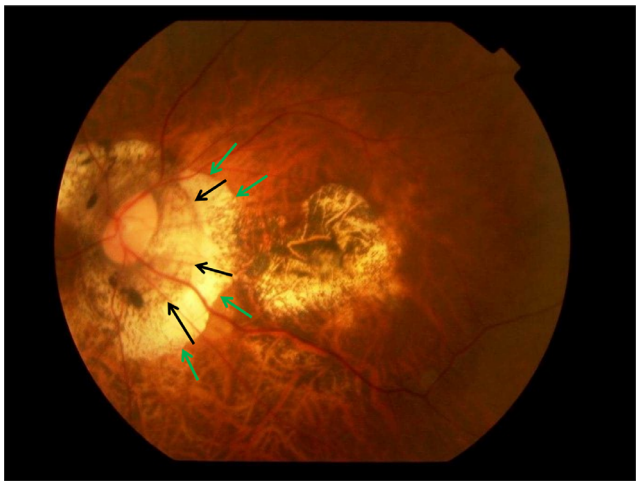

Figure 4. Clinical photograph of a highly myopic eye with parapapillary gamma zone (*green arrows*) and parapapillary delta zone (*black arrows*).

The parapapillary delta zone is defined as a zone within the gamma zone characterized by an elongated and thinned peripapillary scleral flange (Fig. 4).[17,40,43] The posterior sclera physiologically splits into an outer part, continuing into the optic nerve dura mater, and an inner part, continuing into the peripapillary scleral flange.[48,49] The latter connects through the peripapillary border tissue of the peripapillary scleral flange with the lamina cribrosa and forms the anterior border of the orbital cerebrospinal fluid space. The parapapillary beta zone is defined as the region around the ONH with an absence of RPE and with the presence of BM (such as BM is void of RPE).[2,17] In eyes with a gamma zone, the peripapillary scleral flange is covered only by the retinal nerve fiber layer, the choroidal peripapillary border tissue, and the inner limiting membrane.[17,40,43,50] In eyes without a gamma zone or parapapillary beta zone, the peripapillary scleral flange is covered by the choroid, BM, RPE, and deep and superficial retinal layers. Because the peripapillary scleral flange is the biomechanical anchor of the lamina cribrosa, the high myopia–associated stretching of the peripapillary scleral flange may have consequences for the biomechanics of the lamina cribrosa and may be one of the reasons for an increased prevalence of glaucomatous or glaucoma-like optic nerve damage in high myopia. Correspondingly, studies have shown that a large secondary macrodisc and a large delta zone are factors associated clinically with a greater prevalence of glaucomatous or glaucoma-like optic nerve damage.[17,37,40,51,52]

The axial elongation-related enlargement of the BMO and enlargement of gamma zone and delta zone lead to an enlargement of the blind spot in the visual field. The resulting scotoma is absolute because retinal photoreceptors are absent in these regions.

Arterial Circle of Zinn–Haller

The arterial circle of Zinn–Haller is located at the junction of the optic nerve dura mater and the posterior sclera at the

peripheral end of the peripapillary scleral flange.[53] The arterial circle of Zinn–Haller serves to nourish the ONH, including the lamina cribrosa. If visible upon ophthalmoscopy, the arterial circle marks the border between the delta zone and the rest of gamma zone.[17] Elongation of the delta zone leads to an increased distance between the arterial circle and the lamina cribrosa. Consequences of this increased distance between the blood supply and lamina cribrosa could be an additional reason for an increased prevalence of glaucomatous or glaucoma-like optic nerve damage in high myopia.

Peripapillary Border Tissue

Within the ONH canal, the peripapillary choroid and the peripapillary scleral flange are separated from the intrapapillary compartment by the peripapillary border tissue of the choroid ("Jacoby") and of the peripapillary scleral flange ("Elschnig") (Fig. 2).[50,54,55] The border tissue of the peripapillary scleral flange is a continuation of the optic nerve pia mater and continues into the choroidal border tissue, which connects to the end of BM.[17,50] Because the peripapillary scleral flange border tissue perpendicularly crisscrosses with the collagen fibers of the peripapillary scleral flange, and because it is connected through the choroidal border tissue with the BM, the peripapillary scleral flange border tissue supports a biomechanical stabilization of the lamina cribrosa in the sagittal direction. The choroidal border tissue separates the intrachoroidal compartment, in which, owing to fenestrations of the choriocapillaris, fluorescein and albumin leaks into the interstitial space from the intrapapillary compartment. In the latter, the blood vessels are not fenestrated, so that a leakage of albumin or fluorescein physiologically does not occur. The border tissue may, therefore, be the location of the presumed choroid–ONH barrier. Connecting the superficial peripheral end of the lamina cribrosa with the end of BM, the choroidal border tissue elongates by almost the same amount as the end of BM recedes from the optic disc border in eyes with gamma (and delta) zone. The elongation of the choroidal border tissue is accompanied by a corresponding thinning, so that the volume of the choroidal border tissue remains unaffected in eyes with enlarging gamma zone.[50] The elongation and thinning of the choroidal border tissue may lead to its rupture in some eyes with a large gamma zone, so that the end of BM is no longer firmly connected to the ONH. This may be the reason for a curling up of the BM end in myopic eyes with a large gamma zone and may lead to a secondary corrugation of the BM, as can be seen histologically and on optical coherence tomographic (OCT) images.[56]

Beside the scleral spur in the anterior segment of the eye and the vortex veins in the posterior segment, the choroidal border tissue is the only structure connecting the inner sphere of the globe (such as the complex of choroid, BM, RPE, retina, ciliary body, iris, lens, and vitreous body) with the outer shell (such as the sclera and cornea). Because it is connected directly to the extraocular muscles, the sclera undergoes marked rotational acceleration and deceleration movements. The inner sphere underlies the laws of mass inertia so that, in the case of acceleration, it stays back, and, in the case of deceleration, it swings after. The discrepancies in the movements between the outer shell and the inner sphere lead to stress and strain on the scleral spur and the choroidal peripapillary border tissue, which connect the outer shell with the inner sphere. This finding implies that the choroidal peripapillary border tissue has biomechanical importance for the eye. However, it has remained unclear which biomechanical sequels the axial elongation-associated lengthening and thinning of the choroidal peripapillary border tissue may have for the biomechanics of the ONH and for the macula.

The Optic Nerve

High myopia has been identified as a major factor associated with glaucomatous neuropathy, as well as with nonglaucomatous optic nerve damage.[1,37,40,41,57–59] An increased prevalence of glaucomatous optic neuropathy may be due to elongation and thinning of the lamina cribrosa, together with associated intralamina tissue changes and steepening of the translamina cribrosa pressure gradient, elongation and thinning of the peripapillary scleral flange as the biomechanical anchor of the lamina cribrosa, and increased distance between the peripapillary arterial circle of Zinn–Haller and the lamina cribrosa. An increased prevalence of nonglaucomatous optic nerve damage in highly myopic eyes may be due to the increased distance from the retinal ganglion cell bodies to the optic disc, leading to a lengthening and potential stretching of the retinal nerve fibers.[17,59] The increased distance between the retinal ganglion cell bodies and the optic disc is due to the lengthening of the retina in association with the axial elongation and development and enlargement of gamma zone, leading to an increased fovea–optic disc distance.[24,60]

It has remained unclear whether moderate myopia is a risk factor for glaucomatous optic neuropathy.[61–64] Moderate myopia has not been described to be a risk factor for nonglaucomatous optic nerve damage.

Retina

Axial ocular elongation leads to an increase in ocular circumference. According to a recent histomorphometric study in enucleated human eyes, the increase in ocular circumference is, to a minor part, associated with an increase in the length of the ciliary body (pars plicata and pars plana combined), and to a major part, associated with elongation of the retina, such as an increased distance between the ora serrata and optic disc and macula.[60] For each mm increase in axial length, retinal length, measured from the ora serrata to the optic disc, increased by 0.73 mm (95% confidence interval–0.65, 0.81), and the ciliary body length, measured from the scleral spur to the ora serrata, increased by 0.16 mm (95% confidence interval, 0.12–0.20).[60] Retinal length and ciliary body length were correlated with each other, with an increase of ciliary body length by 0.12 mm (95% confidence interval, 0.07–0.17) for each millimeter increase in retinal length. These findings agree with previous observations that myopic globe enlargement mainly affects the axial eye diameter, whereas horizontal and vertical equatorial eye diameters increase by a markedly lower amount.[4–11]

Histomorphometric measurements show that photoreceptor density in association with axial length decreases most markedly in the retroequatorial region, followed by the equatorial region, and finally the ora serrata.[12] As discussed elsewhere in this article, these findings suggest that axial elongation takes place predominantly in the retroequatorial

Investigative Ophthalmology & Visual Science

region, followed by the equatorial region, and finally the ora serrata. Correspondingly, the total retinal thickness measured in the equatorial and retroequatorial regions decreases with longer axial length, whereas retinal thickness in the macular region is not related, or is not markedly related, to the axial length.[13] In clinical studies, a thinner macular retinal outer nuclear layer, as a surrogate for a lower photoreceptor density, has been shown to be associated with longer axial length after correcting for parameters, such as age, sex, disc–fovea distance, and subfoveal choroidal thickness.[12,70] Correspondingly, studies applying adaptive optics scanning laser ophthalmoscopy revealed that the foveal cone mosaic expands with a longer axial length.[71–75] It has remained unclear whether the cone angular sampling density (measured in cones per degree squared) increases, decreases, or is not associated with axial length.[71–75] Generally, one may assume that myopes likely have the same number of photoreceptors and RPE cells as nonmyopic individuals. However, the photoreceptors are spread out over an axial elongation-related larger inner surface area in myopic eyes, so that their overall mean density decreases with a longer axial length. In the fovea, however, the photoreceptor density has not been reported to decrease markedly with a longer axial length. This finding is paralleled by observations that other morphological structures of the fovea, such as the thickness of BM and the density of the foveal RPE cells, are not markedly, or not at all, correlated with axial length.

From a clinical point of view, the myopia-associated decrease in photoreceptor density in the retroequatorial and equatorial regions may cause directly a decrease in spatial resolution and, in association with a potentially decreased density of cells of the inner nuclear layer and retinal ganglion cell layer, an enlargement of receptive fields. These assumptions fit with the clinical observation of a concentric constriction of the visual field in highly myopic eyes.[76] In that context, one may also have to consider that the increased length of the optical axis may lead to a larger projected image on the retina. Clinical studies by Chui et al.[77] have revealed that, at peripheral retinal loci, resolution acuity declines linearly with the magnitude of myopic refractive error. Eyes with a myopic refractive error of −15.0 D, as compared with emmetropic eyes, had twice as much spacing between the retinal receptive units and, thus, 50% of the peripheral resolution acuity.[77] The analysis of ocular expansion patterns using grating acuity data by Chui et al.[77] also concluded that the center of myopic ocular wall expansion is located posterior to the geometric center of the globe. This finding is in accordance with the histomorphometric data on the midperipheral density of the RPE cells and photoreceptors and retinal thickness, as discussed elsewhere in this article.

Other nonpathological changes in the retina associated with axial elongation include lattice degeneration and cobblestone degeneration located in the equatorial and preequatorial regions.[78–81] The prevalence of lattice degeneration increases from emmetropia to moderate myopia with a peak at an axial length of approximately 26.0 to 26.9 mm (or a refractive error of −6.00 to −8.70 D), and decreases toward high myopia and extreme myopia.[79] The prevalence of cobblestone degeneration generally increases with a longer axial length and is the highest in highly myopic eyes. Cobblestones have a bright, whitish color owing to a scarcity or complete absence of melanin in the level of the RPE. In a recent histomorphometric study, the thickness of the BM and the choriocapillaris in cobblestone regions was thinner and, just outside of the cobblestone regions, were thicker than in corresponding regions of eyes without cobblestones.[81] The cobblestone regions showed a firm adhesion between a disorganized retina and a thinned BM, and only few RPE islands, whereas the scleral and total choroid did not show a significant regional thinning. On light microscopy, the BM within the cobblestone regions (except for the RPE islands) seemed to be monolayered, whereas outside of the cobblestone region was double layered. Malignant choroidal melanomas have been found to be correlated spatially with cobblestone degeneration anterior to the tumors,[82] with the authors proposing that a peripheral choroidal blood perfusion insufficiency owing to the choroidal malignant melanomas, as well as owing to other tumors, such as choroidal neve and choroidal metastases, might have caused the cobblestones.

RPE

Similar to the photoreceptors, the underlying RPE also shows a decrease in cell density with longer axial length, most marked in the retroequatorial region.[14] Interestingly, RPE cell density does not decrease, or decreases only to a minor degree, at the posterior pole.[14] The observation that the inverse association between the RPE cell density and axial length was the strongest at the retroequatorial region, followed by the equatorial region, then the ora serrata, and that it was the weakest, if at all present, at the posterior pole, is in line with the notion of a myopic ocular wall enlargement predominantly in the retroequatorial region, whereas the posterior pole itself, except for the development of gamma zone and delta zone, may not be involved in that process primarily.[15] Although not always observed, a slight decrease in the RPE cell density at the posterior pole in association with longer axial length is in alignment with reports on a decrease in foveal cone density with longer axial length.[71–75] The photoreceptor density/RPE cell density ratio may not be affected by the axial length markedly.

BM

Histomorphometric studies on European and Chinese eyes, as well as in a guinea pig model, have shown that the thickness of BM is not related to axial length.[83–85] Even in human eyes with an extreme axial length of more than 30 mm, the foveal BM thickness was similar to eyes with shorter axial lengths. These findings suggest that, because the surface area of BM increases with longer axial length but thickness is constant, the volume of BM increases with longer axial length. This finding is in contrast with the volume of the sclera and choroid, which do not increase in axial elongation.[86,87] The ability of the BM to maintain its thickness suggests that the BM has an active role in the process of axial elongation.

It is important to note that the thickness of BM is just 2 to 4 µm. Moderate changes in BM thickness are difficult to detect by light microscopy. With increasing tensile stress, lengthening occurs, the proportion of which is described by Young's modulus. If one assumes that the BM does not remodel in axially elongating eyes, it should be under some tensile stress. With increasing strain from such a stress, typically some tissue thinning occurs, as described by Poisson's ratio. These considerations may make one assume that there

Investigative Ophthalmology & Visual Science

may be some thinning of the BM, however undetected in previous light microscopy examinations.[84–86]

The distance from the foveola to the optic disc border increases with longer axial length, whereas the distance from the fovea to the border of gamma zone is independent of axial length.[24] The axial length-associated increase in the disc–fovea distance was shown to be due to the development and enlargement of gamma zone, whereas the length of the BM in the macular region was not associated with axial elongation. Correspondingly, the distance between the superior temporal arterial arcade and the inferior temporal arterial arcade in eyes without macular BM defects was found to be independent of axial length, fitting with the notion that the BM in the macular region does not enlarge in axially elongated eyes without BM defects.[88]

Some eyes with marked axial elongation show BM defects in the posterior region and in spatial association with scleral staphylomas.[89] The BM defects were surrounded by a larger area without RPE cells. BM thickness at the edge of the BM defects was not decreased. It has remained unclear whether the BM in axially elongated eyes, in particular in highly myopic eyes, shows changes in its biochemical composition, such as the degree of calcification, as has been shown in eyes with pseudoxanthoma elasticum and AMD.[90–94] This question may also be of interest for the development of lacquer cracks, which may be the ophthalmoscopic equivalent of linear defects in the RPE layer and, in some eyes, of the underlying BM.[95–98] The defects in the RPE layer and in the BM in the macular region correspond, owing to the absence of RPE cells, with an absolute scotoma in the visual field.

Fovea–Optic Disc Distance

The fovea–optic disc distance increases with longer axial length owing to the development and enlargement of a temporal gamma zone.[24] Because the distance between the superior and inferior temporal vascular arcades is independent of axial length, the angle between the temporal vascular arcade decreases with a longer axial length.[88] This process leads to crowding of the retinal nerve fiber layer in the temporal region of the ONH, and correspondingly, to a relative thinning of the retinal nerve fiber layer in the other regions.[88,99,100] In particular, the location of the peaks of the retinal nerve fiber layer thickness profiles move in the direction toward the temporal position.[99] These changes in the retinal nerve fiber layer thickness profile, occurring in association with an axial elongation-associated decrease in angle kappa (such as the angle between the temporal superior vascular arcade and temporal inferior vascular arcade with the optic disc as the angle vertex) have to be taken into account when diagnosing an optic nerve image based on the retinal nerve fiber layer thickness profile.

The increase in the fovea–optic disc distance leads to an elongation, and potentially stretching, of the retinal nerve fibers running in the papillomacular bundle.[101] This may potentially lead to nonglaucomatous optic nerve damage, and might explain the occurrence of paracentral scotomas in highly myopic eyes in which the macular morphology cannot explain the etiology of paracentral scotomas. Retinal nerve fibers, which primarily run in an arcuate manner from their retinal ganglion cell body to the optic disc, may compensate for the increased distance to the optic disc by taking a straighter course. Correspondingly, retinal vessels take a straighter course toward the optic disc in highly myopic eyes undergoing myopia progression.[101]

Choroid

As shown in clinical studies, the thickness of the choroid decreases with a longer axial length, most markedly in the subfoveal region.[102–104] This decrease in choroidal thickness has been shown to affect the layers of medium and large choroidal vessels primarily, whereas the thickness of the choriocapillaris is not, or is only marginally, associated with a longer axial length.[101] Correspondingly, the ratio of the large choroidal vessel layer and of the medium choroidal vessel layer to total choroidal thickness decreases, and the ratio of the choriocapillaris increases with longer axial length.[101]

In a recent clinical study on non–highly myopic individuals, choriocapillaris flow deficits, as measured by OCT angiography, were shown to be independent of axial length in a multivariable analysis adjusting for age, IOP, serum concentrations of high-density lipoprotein cholesterol, and lower image quality score.[105] Similar results have been reported by others.[106,107] However, the latter two studies did not correct for image magnification effects related to axial length. In an investigation conducted by Jiang et al.,[108] the overall vascular density in the choriocapillaris did not vary between highly myopic and non–highly myopic individuals. In contrast, one study reported that choroidal vascularity and choriocapillaris blood perfusion, as measured by OCT angiography, decreased with longer axial length and with choroidal thinning.[109] Similarly, in a study applying swept-source OCT angiography, a longer axial length in highly myopic eyes correlated with a higher choriocapillaris flow deficit in the perifoveal region, although in the parafoveal and foveal regions such an association was not found.[110]

In approximately 17% of highly myopic individuals, an intrachoroidal parapapillary cavitation (also called suprachoroidal parapapillary cavitation), originally described as a peripapillary detachment, is found.[68] An intrachoroidal parapapillary cavitation is defined as a cleavage between the choroid, connected to the BM, and the sclera in the parapapillary region (Fig. 5).[65–69] This cavitation generally occurs in the inferior to temporal inferior parapapillary region. As described by Spaide et al.,[67] lesions appear ophthalmoscopically as orange-colored regions at the inferior to temporal-inferior ONH border, with a backward bowing of the sclera, and without a deformed configuration of the overlying BM–RPE–retina complex. Posterior outward bowing of the sclera might suggests a posterior excursion of the sclera, and not an anterior displacement of the retina and RPE, as cause for the cavitation.[67] It was also proposed that, owing to a physiological elastic stress–strain relationship, the ability to resist deformation is related to the thickness and composition of the layers involved. IOP-related deformation of the posterior scleral wall would be more marked in the region of the parapapillary gamma zone and delta zone than in other posterior fundus regions, because the overlying tissues in the area of the gamma zone and delta zone are either absent or abnormally thin.[67] Another possibility to explain the development of the choroidal cavitations may be, as discussed elsewhere in this article, that the optic nerve is relatively too short to allow full adduction of a markedly elongated eye.[45,46,69] In adduction of extremely elongated eyes, the optic nerve, presumably the optic nerve dura mater, exerts a pull on the posterior sclera at the merging line of the dura mater with the sclera, such as at the peripheral end of the peripapillary scleral flange. This could lead to a backward pull of the peripapillary sclera and to a secondary cleavage between

Investigative Ophthalmology & Visual Science

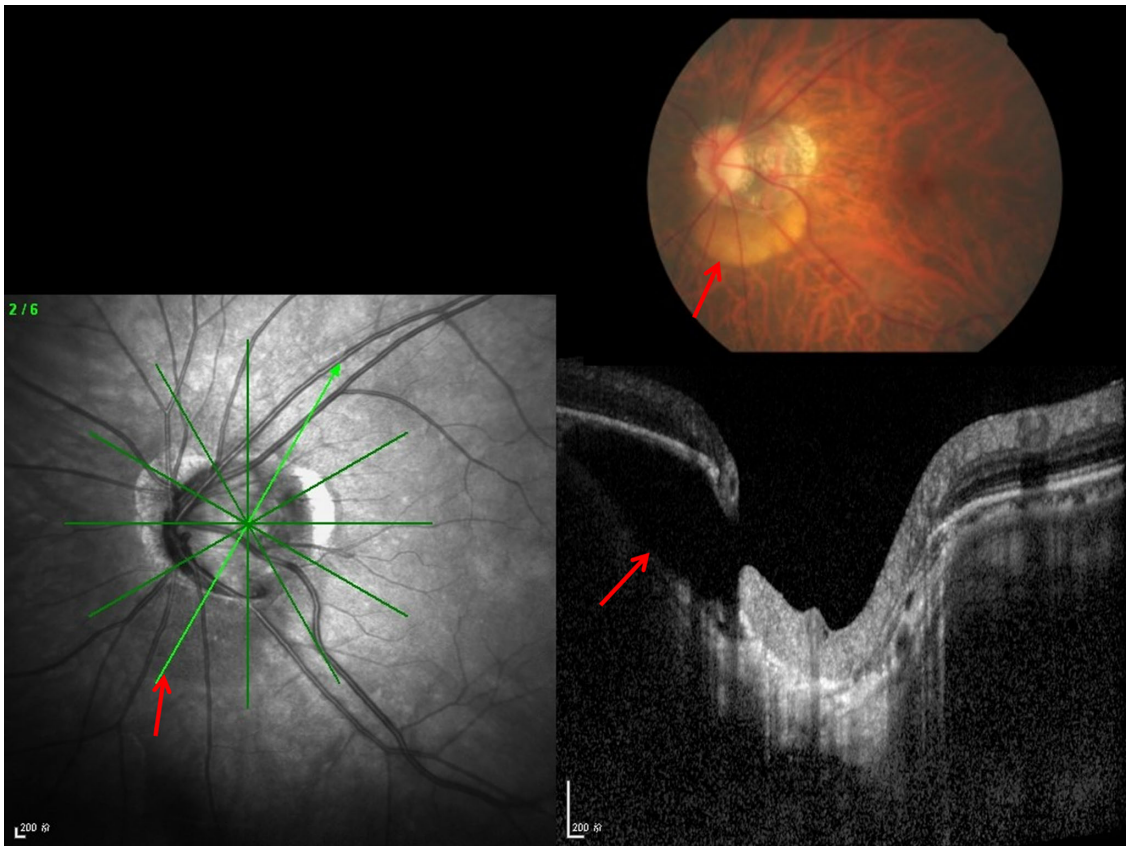

Figure 5. Clinical and optical tomographic image of a parapapillary intrachoroidal cavitation.

the sclera and the choroid, which is adherent to the BM. A suprachoroidal parapapillary cavitation may not be considered pathological, because it is not accompanied by functional deficits generally and has not been reported to be a risk factor for myopia-related pathologies.[68] For details on how myopia control treatments impact the choroid, see the IMI—dynamic choroid white paper.[111]

Sclera

In the process of axial elongation, the sclera undergoes significant remodeling. Its thickness decreases with a longer axial length, most markedly at the posterior pole, and least markedly at the ora serrata and anterior to the ora serrata.[4,112–114] Histomorphological studies have shown that the cross-sectional area and volume of the sclera is not correlated with axial length or age in individuals ages 3 years and older, whereas in children ages 2 years and younger, the scleral cross-sectional area and volume increase with age.[86,87]

The remodeling of the sclera is accompanied by, or induced by, changes in extracellular matrix (ECM) composition and in scleral fibroblasts.[115–135] The sclera is formed by a dense, fibrous, viscoelastic connective tissue that includes irregularly arranged collagen fibrils with proteoglycans and noncollagenous glycoproteins located between the fibrils. Scleral fibroblasts produce the collagen and other components of the ECM. Studies have reported that axial elongation may be associated with active scleral remodeling, contributing to a weakened scleral matrix.[118] As evidence of early scleral remodeling, increases in scleral metabolism and scleral elasticity were observed in tree shrew eyes while undergoing experimental myopia and recovery.[115,116,121] From a biomechanical point of view, investigations of tree shrews revealed that the ratio of tissue extension in relationship to time (such as scleral creep rate) increased in eyes undergoing myopia development and decreased during recovery, when the myopia regressed.[121] These biomechanical changes were considered to be associated with scleral myofibroblasts-induced alterations of the scleral ECM. Changes in the morphological composition of the sclera in myopia has been further demonstrated by Curtin et al.[135] using electron microscopy. The sclera of myopic eyes showed a predominantly lamellar, collagen fiber bundle arrangement, a decrease in the fibril diameter, a larger range in fibril diameters, a higher number of unusual star-shaped fibrils, and a higher count of fibril groups with uniform and very fine diameters compared to emmetropic eyes.[135]

Tissue stress and tissue growth factors, including TGF-β, influence myofibroblasts. Myofibroblasts are differentiated fibroblasts that express α-smooth muscle actin. Correspondingly, the expression of tissue inhibitor of metalloproteinase-2 was decreased in the sclera of tree shrew eyes developing experimental myopia.[127] When tissue inhibitor of metalloproteinase-2 was added exogenously, myopia development and axial elongation significantly decreased, and posterior scleral collagen degradation was inhibited.[125,127]

In a study performing a genome wide association study for highly myopic patients, four Kyoto Encyclopedia of Genes and Genomes signaling pathways, including one for amphetamine addiction, ECM receptor interaction, neuroactive ligand receptor interaction, and regulation of actin cytoskeleton pathways, were associated with

Investigative Ophthalmology & Visual Science

high myopia, and the hypoxia-induing factor-1α signaling pathway was related with high myopia of more than –10.0 D.[132] These results agree with the observation that the hypoxia-signaling, the eIF2-signaling, and mammalian target of rapamycin signaling pathways were activated in a murine model of myopia.[133] Additionally, these results support results of other studies in which experimental myopia in mice and guinea pigs was shown to be related with an hypoxia-induing factor-1α up-regulation in the sclera. Similarly, in human scleral fibroblasts, exposure to hypoxia induced transdifferentiation of myofibroblasts with down-regulation of type I collagen. In another clinical study on highly myopic patients, the examination of sclera-related gene polymorphisms showed that, in particular, polymorphisms of TGF-β 2 were related with myopia so that TGF-β 2 may be an important element in the process of scleral remodeling.[134]

It has remained unclear whether the axial elongation–associated changes in the sclera are alterations primarily leading to axial elongation, or whether an elongation of intraocular tissues develops first with the scleral changes occurring in a secondary manner. It is hypothesized that signaling pathways involved in myopic scleral remodeling involve dopamine, retinoic acid, and adenosine. For recent comprehensive reviews, see Summers et al. (2021)[136] and Brown et al. (2022).[137]

Vitreous

With a longer axial length, macromolecules of the vitreous undergo alterations, the viscosity of the vitreous body decreases, and the prevalence of posterior vitreous detachment increases.[138–142] Although only 2% of the vitreous body consists of macromolecules, they are of high importance for the transparency, gel state, and physiologic function of the vitreous body.[142] An early study of human eyes reported that the myopic vitreous has decreased the protein concentration, collagen content, and hyaluronate concentration than the vitreous of emmetropic eyes.[143] A more recent study in a mouse model of myopia showed that vitreous potassium, sodium, and chloride decrease.[144] With a longer axial length, as well as advancing age, these physiological changes lead to degeneration of the collagen fibrils within the vitreous body and a gel liquefaction of the fibril–hyaluronic acid association, so that vitreous opacities develop, and, eventually, a detachment of the posterior vitreous from the inner limiting membrane of the posterior retina and of the ONH occurs. In some cases, after a posterior vitreous detachment, condensation and adhesion of the posterior vitreous body at the ONH, called the Martegiani ring, is perceived as a large floater. If clinically significant, the vitreous floater induces a reduction in quality of vision. This condition has been termed "vision-degrading myodesopsia."[142] In some highly myopic eyes, the posterior vitreous detachment can be incomplete, with vitreous cortex remaining on the macula.[139]

Anterior Segment

Myopic axial elongation–associated changes in the anterior segment as compared with those in the posterior segment are less marked. The dimensions of the cornea with respect to its thickness and diameter are mostly independent of axial length.[145–147] The anterior corneal curvature radius decreases slightly with axial length in moderately myopic eyes, although it is independent of axial length in highly myopic eyes. The anterior chamber depth and the anterior chamber angle increase with axial length. Correspondingly, a longer axial length is correlated with a lower prevalence and incidence of POAG. The lens thickness decreases with longer axial length in moderately myopic eyes, while lens thickness is not related to axial length in highly myopic eyes.

Conclusions

Myopic axial elongation–associated nonpathological changes occur predominantly in the posterior one-half of the eye. Corresponding with a change in the eye shape from a sphere to a prolate ellipsoid, decreases in photoreceptor and RPE cell density and total retinal thickness are most marked at the retroequatorial region, followed by the equatorial region, and least marked at the posterior pole. Thinning of the choroid and sclera is most pronounced at the posterior pole and least pronounced at the ora serrata. Additionally, the sclera undergoes remodeling early in the development of myopia. These changes in choroidal and scleral thickness occur without a change in the choroidal or scleral volume. The thickness of the BM is not correlated with, and the BM volume increases with, a longer axial length. In moderate myopia, the BMO may shift, usually in the direction of the fovea, leading to an overhanging of the BM into the nasal intrapapillary compartment, an absence of the BM in the temporal region (such as parapapillary gamma zone), an ovalization of the disc shape owing to a shortening of the ophthalmoscopically visible horizontal optic disc diameter with a subsequent decrease in the ophthalmoscopic disc size, an elongation of the fovea–optic disc distance (owing to the development of the gamma zone and without an elongation of the macular BM), a decrease in the angle kappa, and a straightening and stretching of the papillomacular retinal blood vessels and retinal nerve fibers. Anatomic characteristics in highly myopic eyes are an enlargement of the BMO with an optic disc enlargement, elongation and thinning of the lamina cribrosa, peripapillary scleral flange (such as the parapapillary delta zone) and the peripapillary choroidal border tissue, and the development of circular gamma and delta zones. Thorough characterization of ocular changes in nonpathological myopia is of importance to better understand mechanisms of myopic axial elongation, pathological structural changes, and psychophysical sequelae of myopia on visual function.

Acknowledgments

Supported by the International Myopia Institute. The publication and dissemination costs of the International Myopia Institute reports were supported by donations from the Brien Holden Vision Institute, Carl Zeiss Vision, CooperVision, Essilor-Luxottica, Hoya, Thea, Alcon and Oculus.

Disclosure: **J.B. Jonas**, myopia control agent (P); **R.F. Spaide**, Topcon Medical Systems (C), Roche (C), Regeneron (C), Heidelberg Engineering (C), Genentech (C), Alson (C), Topcon (R); **L.A. Ostrin**, (N); **N.S. Logan**, CooperVision (F, C), Dopavision (C), Essilor (C), Hoya (F, C), Ocumension (C), SightGlass (F, C); **I. Flitcroft**, CooperVision (C), EssilorLuxottica (C), Johnson & Johnson Vision (C), Vyluma (C), Thea (C), Ocumetra (O), Myopia control monitoring tools and devices (P); **S. Panda-Jonas**, myopia control agent (P)

References

1. Morgan IG, Ohno-Matsui K, Saw SM. Myopia. *Lancet.* 2012;379(9827):1739–1748.
2. Jonas JB, Jonas RA, Bikbov MM, Wang YX, Panda-Jonas S. Myopia: Histology, clinical features, and potential implications for the etiology of axial elongation. *Prog Retin Eye Res.* 2022 Dec 28:101156, doi:10.1016/j.preteyeres.2022.101156. Online ahead of print.
3. Xu L, Wang YX, Wang S, Jonas JB. Definition of high myopia by parapapillary atrophy. The Beijing Eye Study. *Acta Ophthalmol.* 2010;88(8):e350–e351.
4. Heine L. Beiträge zur Anatomie des myopischen Auges. *Arch Augenheilk.* 1899;38:277–290.
5. Meyer-Schwickerath G,, Gerke E. Biometric studies of the eyeball and retinal detachment. *Br J Ophthalmol.* 1984;68(1):29–31.
6. Cheng HM, Singh OS, Kwong KK, Xiong J, Woods BT, Brady TJ. Shape of the myopic eye as seen with high resolution magnetic resonance imaging. *Optom Vis Sci.* 1992;69(9):698–701.
7. Jonas JB, Ohno-Matsui K, Holbach L, Panda-Jonas S. Association between axial length and horizontal and vertical globe diameters. *Graefes Arch Clin Exp Ophthalmol.* 2017;255(2):237–242.
8. Atchison DA, Jones CE, Schmid KL, et al. Eye shape in emmetropia and myopia. *Invest Ophthalmol Vis Sci.* 2004;45(10):3380–3386.
9. Guo X, Xiao O, Chen Y, Wu H, Chen L, Morgan IG, He M. Three-dimensional eye shape, myopic maculopathy, and visual acuity: The Zhongshan Ophthalmic Center-Brien Holden Vision Institute High Myopia Cohort Study. *Ophthalmology.* 2017;124(5):679–687.
10. Logan NS, Gilmartin B, Wildsoet CF, Dunne MC. Posterior retinal contour in adult human anisomyopia. *Invest Ophthalmol Vis Sci.* 2004;45(7):2152–2162.
11. Matsumura S, Kuo AN, Saw SM. An update of eye shape and myopia. *Eye Contact Lens.* 2019;45(5):279–285.
12. Panda-Jonas S, Jonas JB, Jonas RA. Photoreceptor density in relation to axial length and retinal location in human eyes. *Sci Rep.* 2022;12(1):21371.
13. Jonas JB, Xu L, Wei WB, et al. Retinal thickness and axial length. *Invest Ophthalmol Vis Sci.* 2016;57(4):1791–1797.
14. Jonas JB, Ohno-Matsui K, Holbach L, Panda-Jonas S. Retinal pigment epithelium cell density in relationship to axial length in human eyes. *Acta Ophthalmol.* 2017;95(1):e22–e28.
15. Jonas JB, Ohno-Matsui K, Jiang WJ, Panda-Jonas S. Bruch membrane and the mechanism of myopization: A new theory. *Retina.* 2017;37(8):1428–1440.
16. Zhang Q, Xu L, Wei WB, Wang YX, Jonas JB. Size and shape of Bruch's membrane opening in relationship to axial length, gamma zone and macular Bruch's membrane defects. *Invest Ophthalmol Vis Sci.* 2019;60(7):2591–2598.
17. Wang YX, Panda-Jonas S, Jonas JB. Optic nerve head anatomy in myopia and glaucoma, including parapapillary zones alpha, beta, gamma and delta: Histology and clinical features. *Prog Retin Eye Res.* 2021;83:100933.
18. Smith EL, 3rd, Hung LF, Huang J, Blasdel TL, Humbird TL, Bockhorst KH. Effects of optical defocus on refractive development in monkeys: Evidence for local, regionally selective mechanisms. *Invest Ophthalmol Vis Sci.* 2010;51(8):3864–3873.
19. Smith EL, 3rd. Prentice Award Lecture 2010: A case for peripheral optical treatment strategies for myopia. *Optom Vis Sci.* 2011;88(9):1029–1044.
20. Benavente-Pérez A, Nour A, Troilo D. Axial eye growth and refractive error development can be modified by exposing the peripheral retina to relative myopic or hyperopic defocus. *Invest Ophthalmol Vis Sci.* 2014;55:6765–6773.
21. Hasebe S, Jun J, Varnas SR. Myopia control with positively aspherized progressive addition lenses: A 2-year, multicenter, randomized, controlled trial. *Invest Ophthalmol Vis Sci.* 2014;55(10):7177–7188.
22. Jonas JB, Zhang Q, Xu L, Wei WB, Jonas RA, Wang YX. Change in the ophthalmoscopical optic disc size and shape in a 10-year follow-up: The Beijing Eye Study 2001-2011. *Br J Ophthalmol.* 2023;107(2):283–288. *2021 Sep 2:bjophthalmol-2021-319632*, doi:10.1136/bjophthalmol-2021-319632. *Online ahead of print.*
23. Reis AS, O'Leary N, Yang H, et al. Influence of clinically invisible, but optical coherence tomography detected, optic disc margin anatomy on neuroretinal rim evaluation. *Invest Ophthalmol Vis Sci.* 2012;53(4):1852–1860.
24. Jonas RA, Wang YX, Yang H, et al. Optic disc - Fovea distance, axial length and parapapillary zones. The Beijing Eye Study 2011. *PloS One.* 2015;10(9):e0138701.
25. Jonas JB, Müller-Bergh JA, Schlötzer-Schrehardt UM, Naumann GOH. Histomorphometry of the human optic nerve. *Invest Ophthalmol Vis Sci.* 1990;31(4):736–744
26. Jonas JB, Mardin CY, Schlötzer-Schrehardt U, Naumann GOH. Morphometry of the human lamina cribrosa surface. *Invest Ophthalmol Vis Sci.* 1991;32(2):401–405.
27. Jonas JB, Fernández MC. Shape of the neuroretinal rim and position of the central retinal vessels in glaucoma. *Br J Ophthalmol.* 1994;78(2):99–102.
28. Jonas JB, Gusek GC, Naumann GO. Optic disc, cup and neuroretinal rim size, configuration and correlations in normal eyes. *Invest Ophthalmol Vis Sci.* 1988;29(7):1151–1158.
29. Kim TW, Kim M, Weinreb RN, Woo SJ, Park KH, Hwang JM. Optic disc change with incipient myopia of childhood. *Ophthalmology.* 2012;119(1):21–26.
30. Samarawickrama C, Mitchell P, Tong L, Gazzard G, Lim L, Wong TY, Saw SM. Myopia-related optic disc and retinal changes in adolescent children from Singapore. *Ophthalmology.* 2011;118(10):2050–2057.
31. Guo Y, Liu LJ, Tang P, et al. Parapapillary gamma zone and progression of myopia in school children: The Beijing Children Eye Study. *Invest Ophthalmol Vis Sci.* 2018;59(3):1609–1616.
32. Dai Y, Jonas JB, Ling Z, Sun X. Ophthalmoscopic-perspectively distorted optic disc diameters and real disc diameters. *Invest Ophthalmol Vis Sci.* 2015;56(12):7076–7083.
33. Jonas JB, Gusek GC, Naumann GOH. Optic disk morphometry in high myopia. *Graefes Arch Clin Exp Ophthalmol.* 1988;226(6):587–590.
34. Xu L, Li Y, Wang S, Wang Y, Wang Y, Jonas JB. Characteristics of highly myopic eyes. The Beijing Eye Study. *Ophthalmology.* 2007;114(1):121–126.
35. Jonas JB, Berenshtein E, Holbach L. Lamina cribrosa thickness and spatial relationships between intraocular space and cerebrospinal fluid space in highly myopic eyes. *Invest Ophthalmol Vis Sci.* 2004;45(8):2660–2665.
36. Jonas JB, Berenshtein E, Holbach L. Anatomic relationship between lamina cribrosa, intraocular space, and cerebrospinal fluid space. *Invest Ophthalmol Vis Sci.* 2003;44(12):5189–5195.
37. Xu L, Wang Y, Wang S, Wang Y, Jonas JB. High myopia and glaucoma susceptibility. The Beijing Eye Study. *Ophthalmology.* 2007;114(2):216–220.
38. Ren R, Jonas JB, Tian G, et al. Cerebrospinal fluid pressure in glaucoma. A prospective study. *Ophthalmology.* 2010;117(2):259–266.

39. Jonas JB, Wang N, Yang D. Translamina cribrosa pressure difference as potential element in the pathogenesis of glaucomatous optic neuropathy. *Asia Pac J Ophthalmol (Phila).* 2016;5(1):5–10.
40. Jonas JB, Weber P, Nagaoka N, Ohno-Matsui K. Glaucoma in high myopia and parapapillary delta zone. *PLoS One.* 2017;12(4):e0175120.
41. Wang YX, Yang H, Wei CC, Xu L, Wei WB, Jonas JB. High myopia as risk factor for the 10-year incidence of open-angle glaucoma in the Beijing Eye Study. *Br J Ophthalmol.* 2022 Feb 22:bjophthalmol-2021-320644, doi:10.1136/bjophthalmol-2021-320644. Online ahead of print.
42. Tan NYQ, Sng CCA, Jonas JB, Wong TY, Jansonius NM, Ang M. Glaucoma in myopia: Diagnostic dilemmas. *Br J Ophthalmol.* 2019;103(10):1347–1355.
43. Jonas JB, Jonas SB, Jonas RA, et al. Parapapillary atrophy: Histological gamma zone and delta zone. *PLoS One.* 2012;7(10):e47237.
44. Jonas JB, Zhang Q, Xu L, Wei WB, Jonas RA, Wang YX. Parapapillary gamma zone enlargement in a 10-year follow-up. The Beijing Eye Study 2001-2011. *Eye (Lond).* 2023;37(3):524–530. 2022 Feb 23, doi:10.1038/s41433-022-01978-8. *Online ahead of print.*
45. Demer JL. Optic nerve sheath as a novel mechanical load on the globe in ocular duction. *Invest Ophthalmol Vis Sci.* 2016;57(4):1826–1838.
46. Wang X, Rumpel H, Lim WE, et al. Finite element analysis predicts large optic nerve head strains during horizontal eye movements. *Invest Ophthalmol Vis Sci.* 2016;57(6):2452–2462.
47. Lee KM, Choung HK, Kim M, Oh S, Kim SH. Positional change of optic nerve head vasculature during axial elongation as evidence of lamina cribrosa shifting: Boramae Myopia Cohort Study Report 2. *Ophthalmology.* 2018;125(8):1224–1233.
48. Dichtl A, Jonas JB, Naumann GOH. Histomorphometry of the optic disc in highly myopic eyes with glaucoma. *Br J Ophthalmol.* 1998;82(3):286–289.
49. Ren R, Wang N, Li B, et al. Lamina cribrosa and peripapillary sclera histomorphometry in normal and advanced glaucomatous Chinese eyes with normal and elongated axial length. *Invest Ophthalmol Vis Sci.* 2009;50(5):2175–2184.
50. Jonas RA, Holbach L. Peripapillary border tissue of the choroid and peripapillary scleral flange in human eyes. *Acta Ophthalmol.* 2020;98(1):e43–e49.
51. Nagaoka N, Jonas JB, Morohoshi K, et al. Glaucomatous-type optic discs in high myopia. *PLoS One.* 2015;10(10):e0138825.
52. Chihara E, Liu X, Dong J, et al. Severe myopia as a risk factor for progressive visual field loss in primary open-angle glaucoma. *Ophthalmologica.* 1997;211(2):66–71.
53. Jonas JB, Holbach L, Panda-Jonas S. Peripapillary arterial circle of Zinn-Haller: Location and spatial relationships. *PLoS One.* 2013;8(11):e78867.
54. Elschnig A. Der normale Sehnerveneintritt des menschlichen Auges. *Denkschrift der kais Akad der Wiss, Wien, Math.-naturw.* 1901;Kl 70:219–310.
55. Jacoby E. Über die Neuroglia des Sehnerven. *Klin Monatsbl Augenheilk.* 1905;43:129–137.
56. Jonas JB, Jonas RA, Ohno-Matsui K, Holbach L, Panda-Jonas S. Corrugated Bruch's membrane in high myopia. *Acta Ophthalmol.* 2018;96(2):e147–e151.
57. Jonas JB, Wang YX, Dong L, Panda-Jonas S. High myopia and glaucoma-like optic neuropathy. *Asia Pac J Ophthalmol (Phila).* 2020;9(3):234–238.
58. Bikbov MM, Gilmanshin TR, Kazakbaeva GM, et al. Prevalence of myopic maculopathy among adults in a Russian population. *JAMA Netw Open.* 2020;3(3):e200567.
59. Spaide RF, Ohno-Matsui K. Myopic optic neuropathy. In: Spaide RF, Ohno-Matsui K, Yannuzzi LA. *Pathologic Myopia.* New York: Springer; 2021;367–387.
60. Panda-Jonas S, Auffarth GU, Jonas JB, Jonas RA. Elongation of the retina and ciliary body in dependence of the sagittal eye diameter. *Invest Ophthalmol Vis Sci.* 2022;63(10):18.
61. Jonas JB, Martus P, Budde WM. Anisometropia and degree of optic nerve damage in chronic open-angle glaucoma. *Am J Ophthalmol.* 2002;134(4):547–551.
62. Marcus MW, de Vries MM, Junoy Montolio FG, Jansonius NM. Myopia as a risk factor for open-angle glaucoma: A systematic review and meta-analysis. *Ophthalmology.* 2011;118(10):1989–1994.e2
63. Suzuki Y, Iwase A, Araie M, et al. Risk factors for open-angle glaucoma in a Japanese population: The Tajimi Study. *Ophthalmology.* 2006;113(9):1613–1617.
64. Tham YC, Aung T, Fan Q, et al. Joint Effects of intraocular pressure and myopia on risk of primary open-angle glaucoma: The Singapore Epidemiology of Eye Diseases Study. *Sci Rep.* 2016;6:19320.
65. Freund KB, Ciardella AP, Yannuzzi LA, et al. Peripapillary detachment in pathologic myopia. *Arch Ophthalmol.* 2003;121(2):197–204.
66. Toranzo J, Cohen SY, Erginay A, Gaudric A. Peripapillary intrachoroidal cavitation in myopia. *Am J Ophthalmol.* 2005;140(4):731–732.
67. Spaide RF, Akiba M, Ohno-Matsui K. Evaluation of peripapillary intrachoroidal cavitation with swept source and enhanced depth imaging optical coherence tomography. *Retina.* 2012;32(6):1037–1044.
68. You QS, Peng XY, Chen CX, Xu L, Jonas JB. Peripapillary intrachoroidal cavitations. The Beijing Eye Study. *PLoS One.* 2013;8(10):e78743.
69. Jonas JB, Dai Y, Panda-Jonas S. Peripapillary suprachoroidal cavitation, parapapillary gamma zone and optic disc rotation due to the biomechanics of the optic nerve dura mater. *Invest Ophthalmol Vis Sci.* 2016;57(10):4373.
70. Chua SYL, Dhillon B, Aslam T, et al. Associations with photoreceptor thickness measures in the UK Biobank. *Sci Rep.* 2019;9(1):19440.
71. Dabir S, Mangalesh S, Schouten JS, et al. Axial length and cone density as assessed with adaptive optics in myopia. *Indian J Ophthalmol.* 2015;63(5):423–426.
72. Wang Y, Bensaid N, Tiruveedhula P, Ma J, Ravikumar S, Roorda A. Human foveal cone photoreceptor topography and its dependence on eye length. *Elife.* 2019;8:e47148.
73. Woog K, Legras R. Distribution of mid-peripheral cones in emmetropic and myopic subjects using adaptive optics flood illumination camera. *Ophthalmic Physiol Opt.* 2019;39(2):94–103.
74. Mirhajianmoghadam H, Jnawali A, Musial G, et al. In vivo assessment of foveal geometry and cone photoreceptor density and spacing in children. *Sci Rep.* 2020;10(1):8942.
75. Eckmann-Hansen C, Hansen MH, Laigaard PP, et al. Cone photoreceptor density in the Copenhagen Child Cohort at age 16-17 years. *Ophthalmic Physiol Opt.* 2021;41(6):1292–1299.
76. Fledelius HC, Jacobsen N, Li XQ, Goldschmidt E. The Longitudinal Danish High Myopia Study, Cohort 1948: At age 66 years visual ability is only occasionally affected by visual field defects. *Acta Ophthalmol.* 2019;97(1):36–43.
77. Chui TY, Yap MK, Chan HH, Thibos LN. Retinal stretching limits peripheral visual acuity in myopia. *Vision Res.* 2005;45(5):593–605.

Investigative Ophthalmology & Visual Science

78. Flaxel CJ, Adelman RA, Bailey ST, et al. Posterior vitreous detachment, retinal breaks, and lattice degeneration Preferred Practice Pattern®. *Ophthalmology*. 2020;127(1):P146–P181.
79. Celorio JM, Pruett RC. Prevalence of lattice degeneration and its relation to axial length in severe myopia. *Am J Ophthalmol*. 1991;111(1):20–23
80. Grossniklaus HE, Green WR. Pathologic findings in pathologic myopia. *Retina* 1992;12:127–133.
81. Jonas SB, Jonas RA, Panda-Jonas S, Jonas JB. Histopathology of myopic cobble stones. *Acta Ophthalmol*. 2022;100(1):111–117.
82. Brown GC, Shields JA. Choroidal melanomas and paving stone degeneration. *Ann Ophthalmol*. 1983;15(8):705–708.
83. Jonas JB, Holbach L, Panda-Jonas S. Bruch's membrane thickness in high myopia. *Acta Ophthalmol*. 2014;92(6):e470–e474.
84. Bai HX, Mao Y, Shen L, et al. Bruch's membrane thickness in relationship to axial length. *PLoS One*. 2017;12(8):e0182080
85. Dong L, Shi XH, Kang YK, et al. Bruch's membrane thickness and retinal pigment epithelium cell density in experimental axial elongation. *Sci Rep*. 2019;9(1):6621.
86. Jonas JB, Holbach L, Panda-Jonas S. Scleral cross section area and volume and axial length. *PLoS One*. 2014;9(3):e93551.
87. Shen L, You QS, Xu X, et al. Scleral and choroidal volume in relation to axial length in infants with retinoblastoma versus adults with malignant melanomas or end-stage glaucoma. *Graefes Arch Clin Exp Ophthalmol*. 2016;254(9):1779–1786.
88. Jonas RA, Wang YX, Yang H, et al. Optic disc-fovea angle: The Beijing Eye Study. *PLoS One*. 2015;10(11):e0141771.
89. Jonas JB, Ohno-Matsui K, Spaide RF, Holbach L, Panda-Jonas S. Macular Bruch's membrane defects and axial length: Association with gamma zone and delta zone in peripapillary region. *Invest Ophthalmol Vis Sci*. 2013;54(2):1295–1302.
90. Jampol LM, Acheson R, Eagle RC, Jr, Serjeant G, O'Grady R. Calcification of Bruch's membrane in angioid streaks with homozygous sickle cell disease. *Arch Ophthalmol*. 1987;105(1):93–98.
91. Spraul CW, Grossniklaus HE. Characteristics of drusen and Bruch's membrane in postmortem eyes with age-related macular degeneration. *Arch Ophthalmol*. 1997;115(2):267–273.
92. Booij JC, Baas DC, Beisekeeva J, Gorgels TG, Bergen AA. The dynamic nature of Bruch's membrane. *Prog Retin Eye Res*. 2010;29(1):1–18.
93. Spaide RF, Jonas JB. Peripapillary atrophy with large dehiscences in Bruch membrane in pseudoexanthoma elasticum. *Retina*. 2015;35(8):1507–1510.
94. Risseeuw S, Bennink E, Poirot MG, et al. A reflectivity measure to quantify Bruch's membrane calcification in patients with pseudoxanthoma elasticum using optical coherence tomography. *Transl Vis Sci Technol*. 2020;9(8):34.
95. Ohno-Matsui K, Tokoro T. The progression of lacquer cracks in pathologic myopia. *Retina*. 1996;16(1):29–37.
96. Xu X, Fang Y, Uramoto K, et al. Clinical features of lacquer cracks in eyes with pathologic myopia. *Retina*. 2019;39(7):1265–1277.
97. Fang Y, Yokoi T, Nagaoka N, et al. Progression of myopic maculopathy during 18-year follow-up. *Ophthalmology*. 2018;125(6):863–877.
98. Jonas JB, Xu L, Wei WB, Jonas RA, Wang YX. Progression and associated factors of lacquer cracks/patchy atrophies in high myopia: The Beijing Eye Study 2001-2011. *Graefes Arch Clin Exp Ophthalmol*. 2022;260(10):3221–3229.
99. Zhang Q, Xu L, Zhao L, Jonas RA, Wang YX, Jonas JB. Peaks of circumpapillary retinal nerve fibre layer and associations in healthy eyes: The Beijing Eye Study 2011. *Br J Ophthalmol*. 2022;106(10):1417–1422.
100. Jonas JB, Yan YN, Zhang Q, et al. Retinal nerve fibre layer thickness in association with gamma zone width and disc-fovea distance. *Acta Ophthalmol*. 2022;100(3):632–639 Jan 25, doi:10.1111/aos.15088. Online ahead of print.
101. Jonas RA, Yan YN, Zhang Q, Wang YX, Jonas JB. Elongation of the disc-fovea distance and retinal vessel straightening in high myopia in a 10-year follow-up of the Beijing eye study. *Sci Rep*. 2021;11(1):9006.
102. Fujiwara T, Imamura Y, Margolis R, Slakter JS, Spaide RF. Enhanced depth imaging optical coherence tomography of the choroid in highly myopic eyes. *Am J Ophthalmol*. 2009;148(3):445–450.
103. Wei WB, Xu L, Jonas JB, et al. Subfoveal choroidal thickness: The Beijing Eye Study. *Ophthalmology*. 2013;120(1):175–180.
104. Xu J, Wang YX, Jiang R, Wei WB, Xu L, Jonas JB. Peripapillary choroidal vascular layers: The Beijing Eye Study. *Acta Ophthalmol*. 2017;95(6):619–628.
105. Cheng W, Song Y, Lin F, et al. Choriocapillaris flow deficits in normal Chinese imaged by swept-source optical coherence tomographic angiography. *Am J Ophthalmol*. 2021;235:143–153.
106. Mo J, Duan A, Chan S, Wang X, Wie W. Vascular flow density in pathological myopia: An optical coherence tomography angiography study. *BMJ Open*. 2017;7(2):e013571.
107. Scherm P, Pettenkofer M, Maier M, Lohmann CP, Feucht N. Choriocapillary blood flow in myopic subjects measured with OCT angiography. *Ophthalmic Surg. Lasers Imaging Retina*. 2019;50(5):e133–e139.
108. Jiang Y, Lou S, Li Y, Chen Y, Lu TC. High myopia and macular vascular density: An optical coherence tomography angiography study. *BMC Ophthalmol*. 2021;21(1):407.
109. Wu H, Zhang G, Shen M, et al. Assessment of choroidal vascularity and choriocapillaris blood perfusion in anisomyopic adults by SS-OCT/OCTA. *Invest Ophthalmol Vis Sci*. 2021;62(1):8.
110. Cheng W, Wang W, Song Y, et al. Axial length and choriocapillaris flow deficits in non-pathological high myopia. *Am J Ophthalmol*. 2022;244:68–78.
111. Ostrin LA, Harb EN, Nickla DL, et al. IMI—the dynamic choroid: New insights, challenges and potential significance for human myopia. *Invest Ophthalmol Vis Sci*. 2023;64(6):4.
112. Olsen TW, Aaberg SY, Geroski DH, Edelhauser HF. Human sclera: Thickness and surface area. *Am J Ophthalmol*. 1998;125(2):237–241.
113. Norman RE, Flanagan JG, Rausch SM, et al. Dimensions of the human sclera: Thickness measurement and regional changes with axial length. *Exp Eye Res*. 2010;90(2):277–284.
114. Vurgese S, Panda-Jonas S, Jonas JB. Sclera thickness in human eyes. *PLoS One*. 2012;7(1):e29692.
115. McBrien NA, Lawlor P, Gentle A. Scleral remodeling during the development of and recovery from axial myopia in the tree shrew. *Invest Ophthalmol Vis Sci*. 2000;41(12):3713–3719.
116. McBrien NA, Cornell LM, Gentle A. Structural and ultrastructural changes to the sclera in a mammalian model of high myopia. *Invest Ophthalmol Vis Sci*. 2001;42(10):2179–2187.

Investigative Ophthalmology & Visual Science

117. McBrien NA, Gentle A. Role of the sclera in the development and pathological complications of myopia. *Prog Retin Eye Res*. 2003;22(3):307–338.
118. Rada JA, Shelton S, Norton TT. The sclera and myopia. *Exp Eye Res*. 2006;82(2):185–200.
119. McBrien NA, Metlapally R, Jobling AI, Gentle A. Expression of collagen-binding integrin receptors in the mammalian sclera and their regulation during the development of myopia. *Invest Ophthalmol Vis Sci*. 2006;47(11):4674–4682.
120. Moring AG, Baker JR, Norton TT. Modulation of glycosaminoglycan levels in tree shrew sclera during lens-induced myopia development and recovery. *Invest Ophthalmol Vis Sci*. 2007;48(7):2947–2956.
121. McBrien NA, Jobling AI, Gentle A. Biomechanics of the sclera in myopia: Extracellular and cellular factors. *Optom Vis Sci*. 2009;86(1):E23–30.
122. Zhou X, Ye J, Willcox MD, et al. Changes in protein profiles of guinea pig sclera during development of form deprivation myopia and recovery. *Mol Vis*. 2010;16:2163–2174.
123. Liu HH, Gentle A, Jobling AI, McBrien NA. Inhibition of matrix metalloproteinase activity in the chick sclera and its effect on myopia development. *Invest Ophthalmol Vis Sci*. 2010.51(6):2865–2871.
124. Frost MR, Norton TT. Alterations in protein expression in tree shrew sclera during development of lens-induced myopia and recovery. *Invest Ophthalmol Vis Sci*. 2012;53(1):322–336.
125. McBrien NA. Regulation of scleral metabolism in myopia and the role of transforming growth factor-beta. *Exp Eye Res*. 2013;114:128–140.
126. Metlapally R, Wildsoet CF. Scleral mechanisms underlying ocular growth and myopia. *Prog Mol Biol Transl Sci*. 2015;134:241–248.
127. Liu HH, Kenning MS, Jobling AI, McBrien NA, Gentle A. Reduced scleral TIMP-2 expression is associated with myopia development: TIMP-2 supplementation stabilizes scleral biomarkers of myopia and limits myopia development. *Invest Ophthalmol Vis Sci*. 2017;58(4):1971–1981.
128. Srinivasalu N, McFadden SA, Medcalf C, et al. Gene expression and pathways underlying form deprivation myopia in the guinea pig sclera. *Invest Ophthalmol Vis Sci*. 2018;59(3):1425–1434.
129. Zi Y, Deng Y, Zhao J, et al. Morphologic and biochemical changes in the retina and sclera induced by form deprivation high myopia in guinea pigs. *BMC Ophthalmol*. 2020;20(1):105.
130. She M, Li B, Li T, Zhou X. Dynamic changes of AREG in the sclera during the development of form-deprivation myopia in guinea pigs. *Curr Eye Res*. 2022;47(3):477–483.
131. Brown DM, Kowalski MA, Paulus QM, et al. Altered structure and function of murine sclera in form-deprivation myopia. *Invest Ophthalmol Vis Sci*. 2022;63(13):13.
132. Zhao F, Zhang D, Zhou Q, et al. Scleral HIF-1α is a prominent regulatory candidate for genetic and environmental interactions in human myopia pathogenesis. *EBioMedicine*. 2020;57:102878.
133. Wu H, Chen W, Zhao F, et al. Scleral hypoxia is a target for myopia control. *Proc Natl Acad Sci USA*. 2018;115(30):E7091–E7100.
134. Lin HJ, Wan L, Tsai Y, et al. Sclera-related gene polymorphisms in high myopia. *Mol Vis*. 2009;15:1655–1663.
135. Curtin BJ, Iwamoto T, Renaldo DP. Normal and staphylomatous sclera of high myopia. An electron microscopic study. *Arch Ophthalmol*. 1979;97(5):912–915.
136. Summers JA, Schaeffel F, Marcos S, Wu H, Tkatchenko AV. Functional integration of eye tissues and refractive eye development: Mechanisms and pathways. *Exp Eye Res*. 2021;209:108693.
137. Brown DM, Mazade R, Clarkson-Townsend D, Hogan K, Datta Roy PM, Pardue MT. Candidate pathways for retina to scleral signaling in refractive eye growth. *Exp Eye Res*. 2022;219:109071.
138. Gilmartin B, Nagra M, Logan NS. Shape of the posterior vitreous chamber in human emmetropia and myopia. *Invest Ophthalmol Vis Sci*. 2013;54(12):7240–7251.
139. Itakura H, Kishi S, Li D, Nitta K, Akiyama H. Vitreous changes in high myopia observed by swept-source optical coherence tomography. *Invest Ophthalmol Vis Sci*. 2014;55(3):1447–1452.
140. Milston R, Madigan MC, Sebag J. Vitreous floaters: Etiology, diagnostics, and management. *Surv Ophthalmol*. 2016;61(2):211–227.
141. She X, Ye X, Chen R, Pan D, Shen L. Characteristics of posterior precortical vitreous pockets and Cloquet's canal in patients with myopia by optical coherence tomography. *Invest Ophthalmol Vis Sci*. 2019;60(14):4882–4888.
142. Sebag J. Vitreous and vision degrading Myodesopsia. *Prog Retin Eye Res*. 2020;79:100847.
143. Berman ER, Michaelson IC. The chemical composition of the human vitreous body as related to age and myopia. *Exp Eye Res*. 1964;3:9–15.
144. Cases O, Obry A, Ben-Yacoub S, et al. Impaired vitreous composition and retinal pigment epithelium function in the FoxG1::LRP2 myopic mice. *Biochim Biophys Acta Mol Basis Dis*. 2017;1863:1242–1254.
145. Yin G, Wang YX, Zheng ZY, et al. Ocular axial length and its associations in Chinese. The Beijing Eye Study. *PLoS One*. 2012;7(8):e43172.
146. Bikbov MM, Kazakbaeva GM, Gilmanshin TR, et al. Axial length and its associations in a Russian population: The Ural Eye and Medical Study. *PLoS One*. 2019;14(2):e0211186.
147. Bikbov MM, Gilmanshin TR, Zainullin RM, et al. Macular pigment optical density and its determinants in a Russian population. The Ural Eye and Medical Study. *Acta Ophthalmol*. 2022;100(8):e1691–e1700.

Investigative Ophthalmology & Visual Science